



Article

Age-Related Fourier-Transform Infrared Spectroscopic Changes in Protein Conformation in an Aging Model of Human Dermal Fibroblasts

Cláudia Martins ^{1,†}, Idália Almeida ^{1,2,†} , Sandra Rebelo ¹ , Sandra Magalhães ^{3,*} and Alexandra Nunes ^{1,‡}

¹ iBiMED—Institute of Biomedicine, Department of Medical Sciences, University of Aveiro, 3810-193 Aveiro, Portugal

² CICECO—Aveiro Institute of Materials, Department of Chemistry, University of Aveiro, 3810-193 Aveiro, Portugal

³ UnIC@RISE—Cardiovascular Research & Development Centre, Department of Surgery and Physiology, Faculty of Medicine, University of Porto, 4200-319 Porto, Portugal

* Correspondence: svmagalhaes@med.up.pt

† These authors contributed equally to this work.

‡ These authors contributed equally to this work.

Abstract: The loss of proteostasis, which results in the accumulation of misfolded proteins, is one of the hallmarks of aging and is frequently associated with the aging process. Fibroblasts are a cellular model widely used in the study of aging and can mimic the loss of proteostasis that occurs in the human body. When studying human aging using fibroblasts, two approaches can be used: fibroblasts from the same donor aged in vitro until senescence or fibroblasts from donors of different ages. A previous study by our group showed that the first approach can be used in the study of aging. Thus, this work aimed to study the spectroscopic profile of human dermal fibroblasts from four donors of different ages using Fourier-transform infrared spectroscopy to identify changes in protein conformation and to compare results with those obtained in the previous study. Partial least squares regression analysis and peak intensity analysis suggested that fibroblasts from older donors were characterized by an increase in the levels of antiparallel β -sheets and a decrease in intermolecular β -sheets, in agreement with our previous results.

Keywords: aging; human dermal fibroblasts; FTIR spectroscopy; protein conformation



Citation: Martins, C.; Almeida, I.; Rebelo, S.; Magalhães, S.; Nunes, A. Age-Related Fourier-Transform Infrared Spectroscopic Changes in Protein Conformation in an Aging Model of Human Dermal Fibroblasts. *Spectrosc. J.* **2023**, *1*, 37–48. <https://doi.org/10.3390/spectroscj1010004>

Academic Editor: Clemens Burda

Received: 6 March 2023

Revised: 14 April 2023

Accepted: 21 April 2023

Published: 24 April 2023



Copyright: © 2023 by the authors. Licensee MDPI, Basel, Switzerland. This article is an open access article distributed under the terms and conditions of the Creative Commons Attribution (CC BY) license (<https://creativecommons.org/licenses/by/4.0/>).

1. Introduction

The aging of the human population that has been reported in the last few decades entails social, economic, and medical problems and leads to the burdening of health systems. In this sense, the study of physiological aging is of huge importance to unravel this complex process and increase the quality of life of the elderly [1].

One of the aging hallmarks is the loss of proteostasis [2], which occurs due to the accumulation of misfolded proteins and the failure of their degradation mechanisms, namely, the ubiquitin–proteasome system (UPS) and the autophagy–lysosome pathway [3,4]. The accumulation of misfolded proteins has deleterious consequences for the cell, as these proteins tend to aggregate, becoming cytotoxic and leading to aging [5–7]. Other important aging hallmarks have also been reported [2], and more recently, the contribution of nuclear envelope dysfunction to the aging process was also described [8].

Due to the obvious ethical and time-consuming problems associated with aging studies in humans, cellular models, namely, human fibroblasts, are a good alternative to study aging, as they present similar characteristics to human aging, namely, replicative senescence and proteostasis loss [9–12]. Although human fibroblast cell models are among the most used cell models for the study of aging, they are simpler than humans, being only a monolayer of one cell type, lacking the extracellular matrix, and consequently not allowing

one to observe the interactions between different cell types, tissues, and organs [11,13]. Nevertheless, the fibroblasts retain representative alterations of the aging process that are related to the biological age of the donors and are easy to obtain and manipulate *in vitro* [10,12,14–17].

In the study of aging using fibroblasts as cellular models, two distinct approaches can be used. One can use fibroblasts that are collected from the same donor, usually a young donor, and age them *in vitro* until cells reach senescence, so that the sequential cell passages can be analyzed and compared. In this case, there is less heterogeneity of results, as the cells are from the same donor and there is less influence of external factors; however, this is a time-consuming process, as the cells need to be cultured until they reach senescence [14,18–22]. The other approach uses fibroblasts from donors of different ages. In this case, there is the influence of external factors, which increases heterogeneity; however, it is a less time-consuming process [14,17,23]. Both approaches have already demonstrated success in the study of the aging process. Regarding fibroblasts from the same donor aged *in vitro*, it was already identified that there are metabolomic changes associated with aging using Fourier-transform infrared (FTIR) spectroscopy, namely, changes regarding proteins [20]. Another metabolomic study using nuclear magnetic resonance (NMR) spectroscopy additionally identified a decrease in phosphocholine, ADP and ATP levels [18]. Furthermore, a previous study in our group revealed that the aging process can be studied using human fibroblasts from a newborn subcultured from passage 3 until passage 17, and, using FTIR spectroscopy, there were detected changes in protein conformation, namely, an increased antiparallel β -sheet conformation and a decrease in proteins in intermolecular β -sheet conformation, as well as a decrease in fibril formation [22]. According to aging studies using fibroblasts from donors of different ages, as far as we are concerned, there are still few studies that are focused on metabolic approaches or changes in protein conformation rather than genetic alterations [17,23].

In this sense, the present study aimed to analyze and compare the spectroscopic profile of human dermal fibroblasts from donors of different ages using FTIR spectroscopy, to contribute to the identification of an age-related protein conformational profile. Furthermore, the results obtained in this study using fibroblasts from donors of different ages were compared with the results obtained with fibroblasts aged *in vitro*.

2. Materials and Methods

2.1. Cell Lines and Cell Culture

Human dermal fibroblast cell lines AG22153, AG10803, AG02222 and AG16102 were obtained from the NIA Aging Cell Culture Repository, Apparently Healthy Collection, Coriell Institute for Medical Research (Camden, NJ, USA). These cell lines were collected from 1-day- and 22-, 49-, and 69-year-old male donors, respectively (Table 1). All of them were cultured in a 1:1 mixture of Dulbecco's modified Eagle's medium (DMEM) and Ham's F-12 Nutrient Mixture (Gibco, Thermo Fisher Scientific, Waltham, MA, USA) supplemented with 10% fetal bovine serum (FBS; Gibco, Thermo Fisher Scientific, Waltham, MA, USA). Cells were maintained at 37 °C with 5% CO₂ in a humidified incubator. Every 3–4 days, cells were washed with phosphate-buffered saline (PBS) and culture medium was changed. When they had reached about 80–90% confluence, cells were subcultured until passage 12 using 0.05% trypsin–EDTA. Flasks were left in a CO₂ incubator for 2 min at 37 °C and then, to stop the trypsinization, complete cell culture medium was added to the flasks. Cells were detached from the flask and centrifuged for 3 min at 1000 rpm at room temperature (RT). After that, the supernatant was discarded and the pellet was resuspended in complete cell culture medium and plated into new flasks [22].

Table 1. Characterization of the human dermal fibroblast cell lines.

Characteristics	AG22153	AG10803	AG02222	AG16102
Age of the donor	1 day old	22 years old	49 years old	69 years old
Passage cells were received	P1	P4	P6	P8
Passage cells were used	P12	P12	P12	P12
Biopsy source	Foreskin	Abdomen	Abdomen	Arm
Gender of the donor	Male	Male	Male	Male
Ethnicity of the donor	White/East Indian	White	White	White

2.2. FTIR Spectroscopy

2.2.1. Sample Preparation

At passage 12, cells were counted and cell viability was assessed using trypan blue, as previously described [24]. Then, two aliquots with 5×10^5 cells each were centrifuged for 3 min, 1000 rpm, RT. Then, culture medium was discarded, cells were washed twice with 1 mL of PBS and centrifuged again for 3 min at 2000 rpm at RT. The supernatant was discarded, and the pellet was kept at -80°C until FTIR analysis. The number of cells used for FTIR was based on a previous study using human fibroblasts and FTIR spectroscopy [22].

The four different cell lines were analyzed in passage 12 using an ATR-FTIR Bruker Alpha Platinum spectrometer (Bruker©, Billerica, MA, USA) coupled with OPUS software (Bruker©, Billerica, MA, USA) in mid-IR range ($4000\text{--}600\text{ cm}^{-1}$), with a resolution of 8 cm^{-1} and 64 co-scans. FTIR spectroscopy was performed in a room with controlled and constant temperature and relative humidity (23°C and 35%, respectively). In sum, 5×10^5 cells were placed in a diamond crystal and air-dried to eliminate the water in the samples.

For each cell line, 9 replicates were acquired. Between readings of each sample, the diamond crystal was cleaned with 70% ethanol and distilled water and a background spectrum was acquired to eliminate possible interference from alterations in room conditions. The FTIR spectra were exported in OPUS format.

2.2.2. Spectra Processing

FTIR spectra were analyzed using Unscrambler X software (V.10.5., Camo Analytics, Oslo, Norway). First, spectra were visualized in a line plot and principal component analysis (PCA) was performed to identify outliers [25–27]. Then, spectra were cut between 1800 and 1500 cm^{-1} . A baseline correction using the baseline offset method and an area normalization correction were applied. After that, spectra were derived using 2nd derivative with the Savitzky–Golay algorithm and 3 smoothing points to resolve overlapping peaks.

2.2.3. Peak Intensity Analysis

As in previous studies, the intensity of specific spectral bands for the four different cell lines was calculated using two different approaches [22,28]. The intensity of peaks assigned to protein secondary structures was calculated using the 2nd derivative spectra factored by -1 , namely, β -sheets (1693 cm^{-1} , 1682 cm^{-1} , and 1628 cm^{-1}) [22,29–34]. The ratio between antiparallel β -sheets and the total of β -sheets was calculated using $I_{1693}/I_{1693+1682+1628}$ and the ratio between intermolecular β -sheets and the total of β -sheets was calculated using $I_{1628}/I_{1693+1682+1628}$.

With a different approach, total protein amount and fibril formation were calculated using the baseline-corrected and area-normalized non-derivative spectra to extract the intensity of amide I and amide II peaks. Total protein amount was calculated using the sum of intensities of amide I and amide II peaks ($I_{1648/51} + I_{1543/46}$), and fibril forma-

tion was calculated using the ratio between amide II and amide I peak intensities (ratio $I_{1543/46}/I_{1648/51}$).

Statistical analysis was performed with GraphPad Prism 9.5.0 software (GraphPad software, San Diego, CA, USA), applying ordinary one-way ANOVA test and Tukey's multiple comparison test, considering the normal distribution of samples. Results are expressed as means \pm standard deviation and were considered statistically significant at p value ≤ 0.05 .

2.2.4. Partial Least Squares Regression Analysis

Preprocessed spectra were analyzed using supervised multivariate partial least squares regression (PLS-R) analysis in the $1800\text{--}1500\text{ cm}^{-1}$ region. The X matrix (predictors) was composed of 2nd derivative spectra and the Y matrix (responses) corresponded to the age of the donor, and it was used to produce a correlation plot between spectral profile and age of the donors. A random intern cross-validation with Kernel PLS algorithm was used. For this region, and after analyzing the plot of cumulative explained variance, PLS-R was built using 2 factors to avoid model overfitting [35,36].

3. Results

In order to identify age-related changes, fibroblasts from 1-day- and 22-, 49-, and 69-year-old donors were analyzed by ATR-FTIR coupled with multivariate analysis.

Firstly, the line plots of baseline and area normalized average spectra of all samples were analyzed (Figure 1). Then, peak intensity analysis and PLS-R analysis were performed in the $1800\text{--}1500\text{ cm}^{-1}$ region of the mid-IR spectra, in order to identify changes that occur at the protein level with aging.

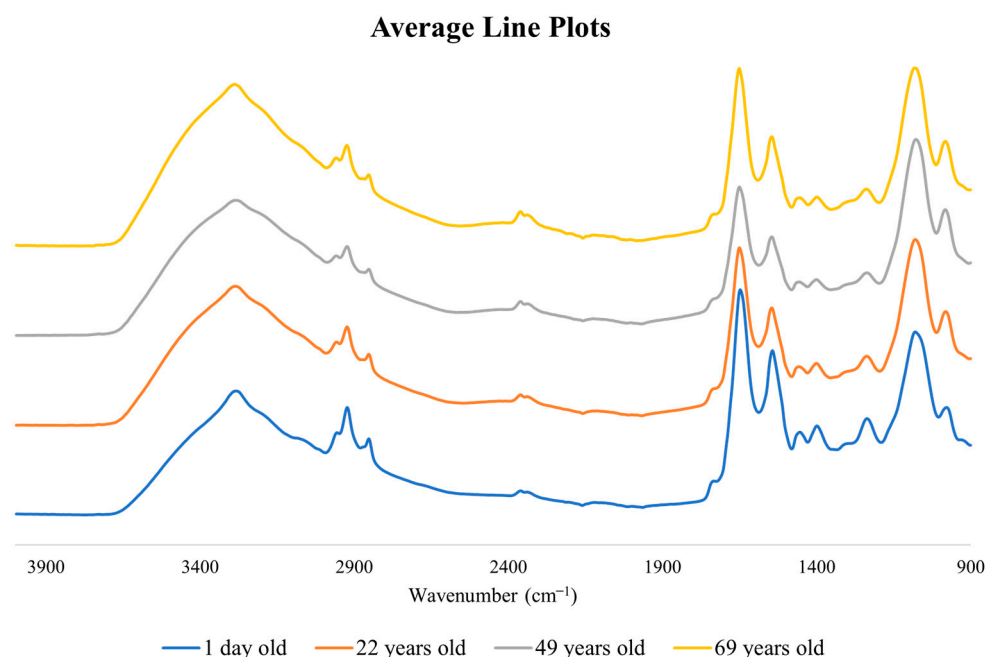


Figure 1. Average FTIR line plot in the mid-infrared region of the spectra. Average baseline and area-normalized line plot of the human dermal fibroblasts of donors with 1-day- and, 22-, 49-, and 69-year-old donors. The box represents the analyzed region of the spectra ($1800\text{--}1500\text{ cm}^{-1}$).

3.1. Peak Intensity Analysis

In order to understand the complexity of the physiological aging process, peak intensity analysis was carried out for the peaks associated with different protein structures at the four time points under study (Figure 2).

Regarding total protein levels (Figure 2A), calculated using the sum of amide I and amide II peaks in the non-derivative spectra, there was a significant decrease in these levels from the 1-day- to the 49-year-old donor, and then an increase to the 69-year-old sample. The ratio between antiparallel β -sheet and β -sheet sum (Figure 2B) constantly increased with age, while the intermolecular β -sheet/ β -sheet sum ratio (Figure 2C) showed a significant decrease with age. Concordantly, the fibril formation ratio (Figure 2D) also decreased with age.

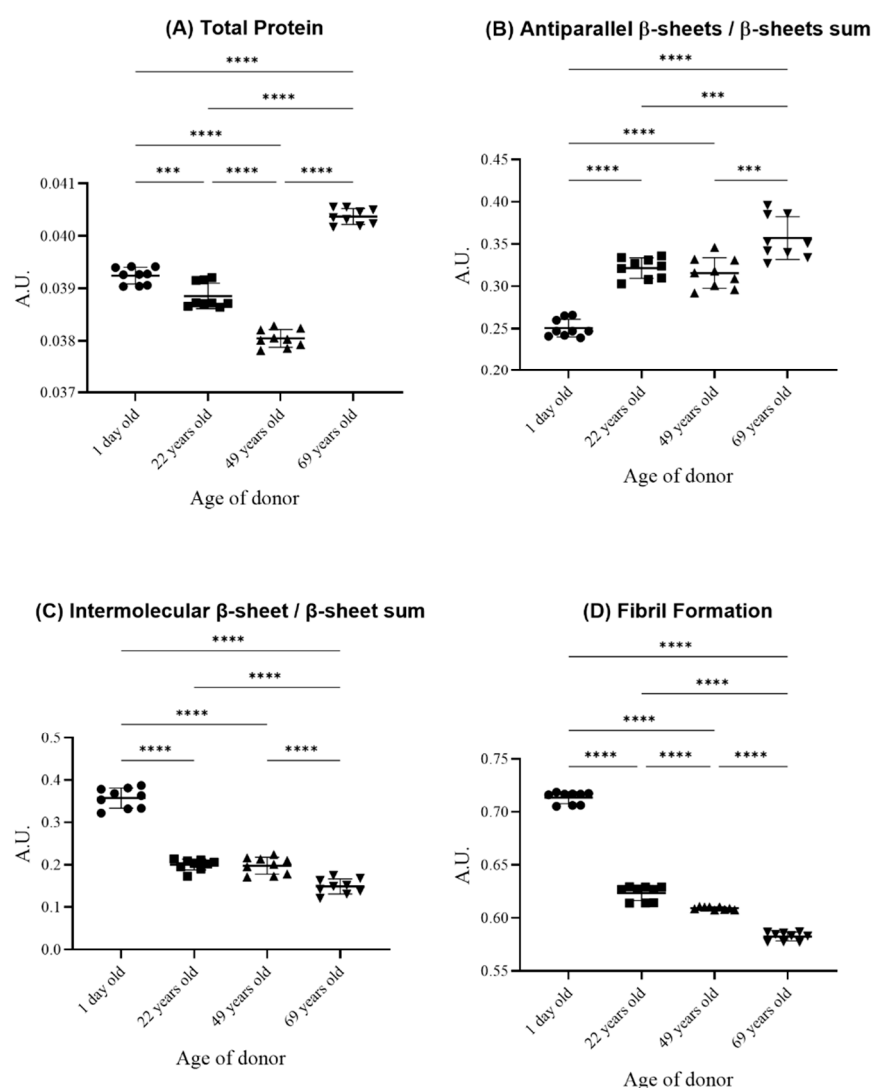


Figure 2. Peak intensity analysis of human dermal fibroblasts of 1-day- and 22-, 49-, and 69-year-old male donors. **(A)** Total protein levels, calculated using the sum of amide I and II peaks, in the non-derived spectra. **(B)** Ratio antiparallel β -sheet/ β -sheet sum ($I_{1693}/I_{1693 + 1682 + 1628}$). **(C)** Ratio intermolecular β -sheet/ β -sheet sum ($I_{1628}/I_{1693 + 1682 + 1628}$). **(D)** Fibril formation, calculated using the ratio between amide II and amide I peaks in the non-derived spectra. Data expressed as means \pm SD. *** $p \leq 0.001$; **** $p \leq 0.0001$. A.U., arbitrary units.

3.2. Spectroscopic Profile of Human Dermal Fibroblasts

A PLS-R analysis was then performed in the $1800\text{--}1500\text{ cm}^{-1}$ region to understand what changes occur with aging at a protein level. In this region of the spectra, two prominent peaks stand out, namely, the amide I and amide II peaks, which can be observed in the non-derived spectra (Figure 3A), and which give important information about proteins and protein structure. In the 2nd derivative spectra (Figure 3B), it is possible to observe the subpeaks of amide I and amide II.

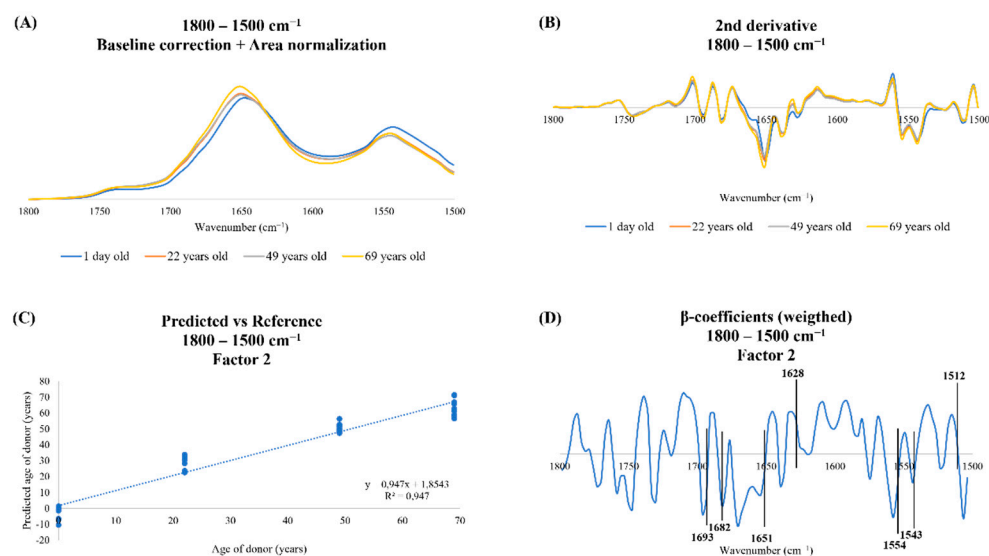


Figure 3. FTIR PLS-R multivariate analysis of the four human dermal fibroblast cell lines in the 1800–1500 cm^{-1} region of the spectra. (A) Average baseline and area normalization-corrected spectra of human fibroblasts in the 1800–1500 cm^{-1} region. (B) Average second derivative corrected spectra of human fibroblasts in the 1800–1500 cm^{-1} region. (C) PLS-R predicted vs. reference plot of factor 2 of the second derivative spectra of human fibroblasts in the 1800–1500 cm^{-1} region. RMSEC (root mean square error of calibration): 6.03; RMSECV (root mean square error of cross-validation): 8.11. (D) β -coefficient plot of factor 2 in the 1800–1500 cm^{-1} region.

Regarding the PLS-R predicted vs. reference plot built with two factors (Figure 3C), it was possible to observe a very high linear and positive relationship between the spectroscopic profile and the age of donors, with a correlation coefficient of 0.97 in the calibration set and 0.95 in the internal cross-validation set [37].

Figure 3D shows the β -coefficient plot of PLS-R in the 1800–1500 cm^{-1} region of the spectra, and the main peaks of these region were identified (Table 2). In this plot, it is possible to observe that younger samples were characterized by antiparallel β -sheets (1693 cm^{-1}) [22,29,30], β -sheets (1682 cm^{-1}) [22,31,32] and α -helices of proteins (1651 cm^{-1}) [22,30,32], whereas older samples were characterized by intermolecular β -sheets (1628 cm^{-1}) [22,33,34].

Table 2. Summary of the main peaks identified in the region 1800–1500 cm^{-1} according to the loading plot (Figure 3D).

Samples	Peak	Biological Meaning	References
younger	1693	antiparallel β -sheets	[22,29,30]
	1682	β -sheets	[22,31,32]
	1651	α -helices	[22,30,32]
	1554	amide II	[38]
	1543		
older	1628	intermolecular β -sheets	[22,33,34]
	1512	amide II	[38]

4. Discussion

Aging is a complex process and varies from one person to another, which makes it necessary for geriatric care to be increasingly personalized rather than generalized [1,39]. Given the difficulty of studying it in humans, it is necessary to use simpler models, such as human dermal fibroblasts [9,40,41].

When studying human physiological aging using fibroblasts, two different approaches can be adopted. Our group has already demonstrated that the aging process can be studied using human dermal fibroblasts from a newborn donor at different cell passages until cells reach senescence [22]. In the present study, we aimed to study the spectroscopic profile of human dermal fibroblasts from 1-day- and 22-, 49-, and 69-year-old donors and compare our results with the results of the previous study.

In this study, the 1800–1500 cm^{-1} region of the mid-IR spectra was analyzed to obtain the maximum information about alterations in the secondary protein conformation with aging [32]. This region of the spectra showed a very high correlation between the spectroscopic profile and the age of donors (Figure 3C) [37]. Firstly, total protein levels were estimated using the sum of amide I and amide II peaks in the non-derived spectra (Figure 2A), as previously described [22,28], and it was observed that it varies with age: until 49 years old, total protein levels decreased, and then increased in fibroblasts from the 69-year-old donor. Previous work by Magalhães et al. (2022) showed that fibroblasts aged in vitro did not follow a linear tendency with increased passage number [22]. Altogether, these oscillations illustrate the complexity of the aging process and might correlate with the hallmark of loss of proteostasis, which leads to changes in both protein synthesis and degradation [4]. To assure homeostasis, the protein network requires a balance of protein synthesis and degradation. However, in the aging process, this balance is affected and an accumulation of damaged proteins is observed, which can lead to cell dysfunction [42]. It has already been shown that the aging process is characterized by a decrease in protein synthesis [42,43], but also by a deregulation in the degradation systems [44,45], showing once again the imbalance of the protein network.

In the PLS-R analysis, it was also possible to observe that younger donors had a peak at 1693 cm^{-1} , corresponding to antiparallel β -sheets, and a peak at 1682 cm^{-1} , corresponding to β -sheets (Figure 3D and Table 2). Peak intensity analysis was performed and confirmed PLS-R data by calculating the ratio between antiparallel β -sheets and total β -sheets, and Figure 2B shows that this ratio increased with age, in concordance with the results of fibroblasts aged in vitro by Magalhães et al. (2022) [22]. As already mentioned above, one of the primary hallmarks of aging is the loss of proteostasis, which leads to protein aggregation [4]. It is known that proteins organized in antiparallel β -sheet conformation are prone to form small toxic oligomers [46]. A previous study using FTIR spectroscopy to analyze protein conformation in control and Alzheimer's disease patients corroborated these results. The authors demonstrated that both fibrils and oligomers have β -sheets, but in different conformations [47]. Oligomers are characterized by antiparallel β -sheets, which cause membrane disruption and/or permeabilization, as they can lead to pore formation in membranes, leading to cell toxicity and death and consequently to aging [47,48].

Regarding intermolecular β -sheets, the β -coefficient plot showed a peak at 1628 cm^{-1} associated with older samples (Figure 3D and Table 2), showing that this peak of the spectra can discriminate between older and younger samples. A peak intensity analysis was performed using the ratio between intermolecular β -sheet and β -sheet sum, and the results showed a decrease with age in this ratio (Figure 2C). These results are in accordance with the results of our previous study, which showed a significant decrease in this ratio in fibroblasts with higher passage number [22]. Intermolecular β -sheets are formed when either parallel or antiparallel β -sheet structures bond through hydrophobic bonds. These structures are known as aggregate prone structures that tend to lead to the formation of fibrils [46,49,50]. Two proteins can interact by hydrophobic forces and form amorphous structures that can subsequently lead to the formation of fibrils [51]. The formation of fibrils alters the function of the proteins that can lose their function or become toxic [7,52]. Besides that, the fibrils are more stable and insoluble, which makes the elimination of these toxic aggregates difficult [7,53]. Furthermore, in aging, UPS is compromised, hindering the elimination of misfolded proteins, which accumulate and aggregate, causing proteostasis failure and contributing to aging [7]. A peak intensity analysis was performed to understand age-related changes in protein conformation. Figure 2D shows that the formation of fibrils

decreased with increasing age, that is, in concordance with the ratio of intermolecular β -sheets, and in concordance with the results obtained by Magalhães et al. (2022) for fibroblasts at higher passage number [22]. Given that aging is characterized by the loss of proteostasis, one would expect that with increasing age, intermolecular β -sheets would increase and there would be higher formation of fibrils. However, a decrease in the ratio between intermolecular β -sheets and total β -sheets was observed in older fibroblasts, as well as a decrease in the fibril formation ratio. Comparing antiparallel and intermolecular β -sheets, there seemed to be a tendency to increased antiparallel β -sheets in older fibroblasts. Besides, the decrease in intermolecular β -sheets and in the fibril formation ratio could be due to a decrease in the formation of proteins in β -sheet conformation with age [22].

In the present study, it was possible to observe that the study of changes in protein conformation with age is plausible using cell cultures of fibroblasts of donors of different ages. As shown in Table 1, dermal fibroblasts from white male donors were used, all in the same passage number. These fibroblasts were obtained from different areas of the body, namely, foreskin in the case of the 1-day-old donor, the abdomen of the 22- and 49-year-old donors and the arm of the 69-year-old donor. It has already been demonstrated that fibroblasts obtained from different regions of the body have similar morphology [54,55], although different studies have already shown that fibroblasts from different anatomical sites present some differences since they can have different embryonic origins [54]. Besides that, it was shown that the proliferation rate, apoptotic rate and migration rate differ in the different dermal fibroblasts, as well as the expression of growth factors [55]. Moreover, the gene expression of fibroblasts from different body parts is different, as well as the composition of the extracellular matrix [54–58]. It is also important to note that the sites from which the fibroblasts were obtained are not all equally exposed to ultraviolet (UV) radiation: fibroblasts from the arm tend to be more exposed to the UV radiation than fibroblasts from the abdomen. This is relevant because chronic exposure to UV radiation causes photoaging and accelerates the appearance of age-associated changes [59,60]. Despite all these stated limitations, it was possible to observe a strong relationship between the spectroscopic profile and age, and that there were spectroscopic alterations associated with protein secondary structure that were characteristic of physiological aging. Besides that, when comparing the results obtained here with the results previously obtained by our research group with fibroblasts from a single donor that were aged in vitro [22], it was possible to observe that the changes in the protein conformation with aging (1800–1500 cm^{-1} region) were similar between the studies. The main alterations observed in aged fibroblasts, in both studies, were an increase in antiparallel β -sheet ratio and a decrease in intermolecular β -sheet ratio and fibril formation, observed in peak intensity analysis using the results obtained with FTIR spectroscopy. These alterations that occurred regarding secondary structure of proteins were in concordance with loss of proteostasis.

Since both approaches have shown similar results in the study of aging, which is the best approach to use? This decision depends on the type of study one intends to conduct. If the objective is to conduct an initial exploratory study, one can consider using fibroblasts from the same donor aged in vitro until senescence, as this approach has less heterogeneity of results and less influence of external factors that alter the aging process. However, this approach is both more expensive and time-consuming, as fibroblasts need to be cultured until they reach senescence [14,18–22]. After the identification of biomarkers in this initial exploratory study, it would be interesting to analyze how the real population fits with these results. For this purpose, fibroblasts from different donors of different ages can be used, thus taking into account the factors that can alter the aging process, from genetic factors to external factors, such as diet or lifestyle [61,62], in a study that would be less time-consuming [14,17,23].

The identification of biomarkers of aging is becoming increasingly important. The goal should be to move towards a more personalized health-care system, with geriatric care becoming more and more effective [63]. The study of omics, from genomics to proteomics or metabolomics, is a great ally to personalized medicine, as it can be useful in identifying

changes that might be useful to, for example, predict and prevent diseases associated with aging or understand which drugs are most suitable for each person, which ultimately might increase the average life expectancy but mainly the quality of life of the elderly [63,64].

The results obtained in this study prove that there are spectroscopic changes associated with the aging process, namely, changes in the secondary conformation of proteins. In the future, it would be interesting to study the metabolome of these cell lines using even more specific metabolomic techniques, namely, NMR and mass spectrometry (MS), in order to possibly corroborate the results obtained here and to identify biomarkers of physiological aging, contributing to personalized medicine in geriatric care.

5. Conclusions

In this study, we aimed to study the aging changes in protein conformation, using human dermal fibroblasts from four donors of different ages (1 day and 22, 49, and 69 years) and FTIR spectroscopy. Besides that, we aimed to compare the results with the results of a previous study in our group with fibroblasts aged in vitro [22]. It was possible to conclude that the spectroscopic results in both studies were similar, and that these two methodological approaches can be used to study age-related changes in proteostasis.

Although these results were in agreement with reported literature, this was an exploratory study in which only four samples collected from donors of different ages were analyzed. This is a limitation of the present work, and we are aware that a higher number of samples in each age under study could increase the significance of the results and decrease the associated error. Furthermore, the fibroblasts were not all obtained from the same region of the body, which might influence the obtained results, as fibroblasts from the same region of the body have similar morphologies but different genetic characteristics and are exposed differently to radiation, which also can cause alterations in the aging process. Despite this, it was possible to identify a relationship between the FTIR spectroscopic profile of the samples and the age of the donors, and it was possible to suggest that this methodological approach can be used in a larger data set in the study of alterations in protein conformation with aging.

This study has demonstrated, once again, the importance of FTIR spectroscopy in the study of aging. This is a simple and fast technique that allows one to trace the spectroscopic profile of a sample, as well as identify aging-associated alterations, when coupled with multivariate analysis. If coupled with a microscope, it is also possible to observe these spectroscopic alterations in living cells [65]. FTIR spectroscopy opens doors to move towards personalized medicine and improve the quality of life of the elderly population.

Author Contributions: Conceptualization, S.M. and A.N.; funding acquisition, S.R. and A.N.; formal analysis, C.M., I.A. and S.M.; investigation, C.M. and I.A.; methodology, S.R., S.M. and A.N.; supervision, S.R., S.M. and A.N.; validation, I.A. and S.M.; visualization, C.M.; writing—original draft, C.M.; writing—review and editing, C.M., I.A., S.R., S.M. and A.N. All authors have read and agreed to the published version of the manuscript.

Funding: This work was supported by Fundação para a Ciência e Tecnologia (FCT) I.P. (PIDDAC), and the European Regional Development Fund (FEDER) (projects UIDB/04501/2020; UIDB/50011/2020; UIDP/50011/2020; CENTRO-01-0145-FEDER-000003 and 2021.07230.BD to IA).

Institutional Review Board Statement: Not applicable.

Informed Consent Statement: Not applicable.

Data Availability Statement: Not applicable.

Conflicts of Interest: The authors declare no conflict of interest.

References

1. Micó, V.; Berninches, L.; Tapia, J.; Daimiel, L. NutrimiRAging: Micromanaging Nutrient Sensing Pathways through Nutrition to Promote Healthy Aging. *Int. J. Mol. Sci.* **2017**, *18*, 915. [[CrossRef](#)] [[PubMed](#)]
2. López-Otín, C.; Blasco, M.A.; Partridge, L.; Serrano, M.; Kroemer, G. Hallmarks of Aging: An Expanding Universe. *Cell* **2023**, *186*, 243–278. [[CrossRef](#)] [[PubMed](#)]
3. Clausen, L.; Abildgaard, A.B.; Gersing, S.K.; Stein, A.; Lindorff-Larsen, K.; Hartmann-Petersen, R. Protein Stability and Degradation in Health and Disease. *Adv. Protein Chem. Struct. Biol.* **2019**, *114*, 61–83. [[CrossRef](#)]
4. Taylor, R.C.; Dillin, A. Aging as an Event of Proteostasis Collapse. *Cold Spring Harb. Perspect. Biol.* **2011**, *3*, a004440. [[CrossRef](#)]
5. Stefani, M.; Dobson, C.M.; Stefani, M.; Dobson, C.M. Protein Aggregation and Aggregate Toxicity: New Insights into Protein Folding, Misfolding Diseases and Biological Evolution. *J. Mol. Med.* **2003**, *81*, 678–699. [[CrossRef](#)]
6. Chiti, F.; Stefani, M.; Taddei, N.; Ramponi, G.; Dobson, C.M. Rationalization of the Effects of Mutations on Peptide and Protein Aggregation Rates. *Nature* **2003**, *424*, 805–808. [[CrossRef](#)]
7. Cuanalo-Contreras, K.; Schulz, J.; Mukherjee, A.; Park, K.W.; Armijo, E.; Soto, C. Extensive Accumulation of Misfolded Protein Aggregates during Natural Aging and Senescence. *Front. Aging Neurosci.* **2023**, *14*, 1090109. [[CrossRef](#)] [[PubMed](#)]
8. Martins, F.; Sousa, J.; Pereira, C.D.; da Cruz e Silva, O.A.B.; Rebelo, S. Nuclear Envelope Dysfunction and Its Contribution to the Aging Process. *Aging Cell* **2020**, *19*, e13143. [[CrossRef](#)] [[PubMed](#)]
9. Lees, H.; Walters, H.; Cox, L.S. Animal and Human Models to Understand Ageing. *Maturitas* **2016**, *93*, 18–27. [[CrossRef](#)] [[PubMed](#)]
10. Cristofalo, V.J.; Beck, J.; Allen, R.G.; Smith, J.R. Cell Senescence: An Evaluation of Replicative Senescence in Culture as a Model for Cell Aging in Situ. *J. Gerontol. Ser. A Biol. Sci. Med. Sci.* **2003**, *58*, 776–781. [[CrossRef](#)] [[PubMed](#)]
11. Lidzbarsky, G.; Gutman, D.; Shekhidem, H.A.; Sharvit, L.; Atzmon, G. Genomic Instabilities, Cellular Senescence, and Aging: In Vitro, In Vivo and Aging-Like Human Syndromes. *Front. Med.* **2018**, *5*, 104. [[CrossRef](#)]
12. Wang, Y.; Chen, S.; Yan, Z.; Pei, M. A Prospect of Cell Immortalization Combined with Matrix Microenvironmental Optimization Strategy for Tissue Engineering and Regeneration. *Cell Biosci.* **2019**, *9*, 7. [[CrossRef](#)]
13. Brunet, A. Old and New Models for the Study of Human Ageing. *Nat. Rev. Mol. Cell Biol.* **2020**, *21*, 491–493. [[CrossRef](#)] [[PubMed](#)]
14. Phipps, S.M.O.; Berletch, J.B.; Andrews, L.G.; Tollefsbol, T.O. Aging Cell Culture: Methods and Observations. *Methods Mol. Biol.* **2007**, *371*, 9–19. [[CrossRef](#)] [[PubMed](#)]
15. Tigges, J.; Krutmann, J.; Fritsche, E.; Haendeler, J.; Schaal, H.; Fischer, J.W.; Kalfalah, F.; Reinke, H.; Reifemberger, G.; Stühler, K.; et al. The Hallmarks of Fibroblast Ageing. *Mech. Ageing Dev.* **2014**, *138*, 26–44. [[CrossRef](#)] [[PubMed](#)]
16. Fleischer, J.G.; Schulte, R.; Tsai, H.H.; Tyagi, S.; Ibarra, A.; Shokhirev, M.N.; Huang, L.; Hetzer, M.W.; Navlakha, S. Predicting Age from the Transcriptome of Human Dermal Fibroblasts. *Genome Biol.* **2018**, *19*, 221. [[CrossRef](#)] [[PubMed](#)]
17. Lagoid, J.C.; Puzzi, M.B. The Effect of Aging in Primary Human Dermal Fibroblasts. *PLoS ONE* **2019**, *14*, e0219165. [[CrossRef](#)]
18. Gey, C.; Seeger, K. Metabolic Changes during Cellular Senescence Investigated by Proton NMR-Spectroscopy. *Mech. Ageing Dev.* **2013**, *134*, 130–138. [[CrossRef](#)] [[PubMed](#)]
19. Eberhardt, K.; Beleites, C.; Marthandan, S.; Matthäus, C.; Diekmann, S.; Popp, J. Raman and Infrared Spectroscopy Distinguishing Replicative Senescent from Proliferating Primary Human Fibroblast Cells by Detecting Spectral Differences Mainly Due to Biomolecular Alterations. *Anal. Chem.* **2017**, *89*, 2937–2947. [[CrossRef](#)]
20. Eberhardt, K.; Matthäus, C.; Marthandan, S.; Diekmann, S.; Popp, J. Raman and Infrared Spectroscopy Reveal That Proliferating and Quiescent Human Fibroblast Cells Age by Biochemically Similar but Not Identical Processes. *PLoS ONE* **2018**, *13*, e0207380. [[CrossRef](#)] [[PubMed](#)]
21. Chan, M.; Yuan, H.; Soifer, I.; Maile, T.M.; Wang, R.Y.; Ireland, A.; O'Brien, J.; Goudeau, J.; Chan, L.; Vijay, T.; et al. Novel Insights from a Multiomics Dissection of the Hayflick Limit. *eLife* **2022**, *11*, e70283. [[CrossRef](#)]
22. Magalhães, S.; Almeida, I.; Pereira, C.D.; Rebelo, S.; Goodfellow, B.J.; Nunes, A. The Long-Term Culture of Human Fibroblasts Reveals a Spectroscopic Signature of Senescence. *Int. J. Mol. Sci.* **2022**, *23*, 5830. [[CrossRef](#)] [[PubMed](#)]
23. Pain, S.; Dezutter, C.; Reymermier, C.; Vogelgesang, B.; Delay, E.; André, V. Age-Related Changes in pro-Opiomelanocortin (POMC) and Related Receptors in Human Epidermis. *Int. J. Cosmet. Sci.* **2010**, *32*, 266–275. [[CrossRef](#)] [[PubMed](#)]
24. Crowley, L.C.; Marfell, B.J.; Christensen, M.E.; Waterhouse, N.J. Measuring Cell Death by Trypan Blue Uptake and Light Microscopy. *Cold Spring Harb. Protoc.* **2016**, *2016*, 643–646. [[CrossRef](#)] [[PubMed](#)]
25. Magalhães, S.; Goodfellow, B.J.; Nunes, A. FTIR Spectroscopy in Biomedical Research: How to Get the Most out of Its Potential. *Appl. Spectrosc. Rev.* **2021**, *56*, 869–907. [[CrossRef](#)]
26. Agahian, F.; Funt, B. Outlier Modeling for Spectral Data Reduction. *J. Opt. Soc. Am.* **2014**, *31*, 1445. [[CrossRef](#)]
27. Nieuwoudt, H.H.; Prior, B.A.; Pretorius, I.S.; Manley, M.; Bauer, F.F. Principal Component Analysis Applied to Fourier Transform Infrared Spectroscopy for the Design of Calibration Sets for Glycerol Prediction Models in Wine and for the Detection and Classification of Outlier Samples. *J. Agric. Food Chem.* **2004**, *52*, 3726–3735. [[CrossRef](#)] [[PubMed](#)]
28. Magalhães, S.; Almeida, I.; Martins, F.; Camões, F.; Soares, A.R.; Goodfellow, B.J.; Rebelo, S.; Nunes, A. FTIR Spectroscopy as a Tool to Study Age-Related Changes in Cardiac and Skeletal Muscle of Female C57BL/6J Mice. *Molecules* **2021**, *26*, 6410. [[CrossRef](#)]
29. Juszczak, P.; Kolodziejczyk, A.S.; Grzonka, Z. FTIR Spectroscopic Studies on Aggregation Process of the Beta-Amyloid 11-28 Fragment and Its Variants. *J. Pept. Sci.* **2009**, *15*, 23–29. [[CrossRef](#)]

30. Mateus, T.; Almeida, I.; Costa, A.; Viegas, D.; Magalhães, S.; Martins, F.; Herdeiro, M.T.; da Cruz e Silva, O.A.B.; Fraga, C.; Alves, I.; et al. Fourier-Transform Infrared Spectroscopy as a Discriminatory Tool for Myotonic Dystrophy Type 1 Metabolism: A Pilot Study. *Int. J. Environ. Res. Public Health* **2021**, *18*, 3800. [CrossRef]
31. Kong, J.; Yu, S. Fourier Transform Infrared Spectroscopic Analysis of Protein Secondary Structures. *Acta Biochim. Biophys. Sin.* **2007**, *39*, 549–559. [CrossRef] [PubMed]
32. Yang, H.; Yang, S.; Kong, J.; Dong, A.; Yu, S. Obtaining Information about Protein Secondary Structures in Aqueous Solution Using Fourier Transform IR Spectroscopy. *Nat. Protoc.* **2015**, *10*, 382–396. [CrossRef] [PubMed]
33. Usoltsev, D.; Sitnikova, V.; Kajava, A.; Uspenskaya, M. FTIR Spectroscopy Study of the Secondary Structure Changes in Human Serum Albumin and Trypsin under Neutral Salts. *Biomolecules* **2020**, *10*, 606. [CrossRef]
34. Sadat, A.; Joye, I.J. Peak Fitting Applied to Fourier Transform Infrared and Raman Spectroscopic Analysis of Proteins. *Appl. Sci.* **2020**, *10*, 5918. [CrossRef]
35. Wang, H.; Ju, A.; Wang, L. Ultraviolet Spectroscopic Detection of Nitrate and Nitrite in Seawater Simultaneously Based on Partial Least Squares. *Molecules* **2021**, *26*, 3685. [CrossRef] [PubMed]
36. Sharaf, Y.A.; Ibrahim, A.E.; El Deeb, S.; Sayed, R.A. Green Chemometric Determination of Cefotaxime Sodium in the Presence of Its Degradation Impurities Using Different Multivariate Data Processing Tools; GAPI and AGREE Greenness Evaluation. *Molecules* **2023**, *28*, 2187. [CrossRef]
37. Glassford, S.E.; Byrne, B.; Kazarian, S.G. Recent Applications of ATR FTIR Spectroscopy and Imaging to Proteins. *Biochim. Biophys. Acta* **2013**, *1834*, 2849–2858. [CrossRef]
38. Asuero, A.G.; Sayago, A.; González, A.G. The Correlation Coefficient: An Overview. *Crit. Rev. Anal. Chem.* **2007**, *36*, 41–59. [CrossRef]
39. Mortality and Life Expectancy Statistics—Statistics Explained. Available online: https://ec.europa.eu/eurostat/statistics-explained/index.php?title=Mortality_and_life_expectancy_statistics#Life_expectancy_at_birth (accessed on 20 June 2022).
40. Mitchell, S.J.; Scheibye-Knudsen, M.; Longo, D.L.; de Cabo, R. Animal Models of Aging Research: Implications for Human Aging and Age-Related Diseases. *Annu. Rev. Anim. Biosci.* **2015**, *3*, 283–303. [CrossRef] [PubMed]
41. Ferrucci, L.; Kuchel, G.A. Heterogeneity of Aging: Individual Risk Factors, Mechanisms, Patient Priorities, and Outcomes. *J. Am. Geriatr. Soc.* **2021**, *69*, 610–612. [CrossRef]
42. Anisimova, A.S.; Alexandrov, A.I.; Makarova, N.E.; Gladyshev, V.N.; Dmitriev, S.E. Protein Synthesis and Quality Control in Aging. *Aging* **2018**, *10*, 4269. [CrossRef] [PubMed]
43. Anisimova, A.S.; Meerson, M.B.; Gerashchenko, M.V.; Kulakovskiy, I.V.; Dmitriev, S.E.; Gladyshev, V.N. Multifaceted Deregulation of Gene Expression and Protein Synthesis with Age. *Proc. Natl. Acad. Sci. USA* **2020**, *117*, 15581–15590. [CrossRef] [PubMed]
44. Vilchez, D.; Saez, I.; Dillin, A. The Role of Protein Clearance Mechanisms in Organismal Ageing and Age-Related Diseases. *Nat. Commun.* **2014**, *5*, 5659. [CrossRef] [PubMed]
45. Frankowska, N.; Lisowska, K.; Witkowski, J.M. Proteolysis Dysfunction in the Process of Aging and Age-Related Diseases. *Front. Aging* **2022**, *3*, 85. [CrossRef]
46. Chiti, F.; Dobson, C.M. Protein Misfolding, Amyloid Formation, and Human Disease: A Summary of Progress Over the Last Decade. *Annu. Rev. Biochem.* **2017**, *86*, 27–68. [CrossRef] [PubMed]
47. Cerf, E.; Sarroukh, R.; Tamamizu-Kato, S.; Breydo, L.; Derclayes, S.; Dufrénes, Y.F.; Narayanaswami, V.; Goormaghtigh, E.; Ruyschaert, J.M.; Raussens, V. Antiparallel Beta-Sheet: A Signature Structure of the Oligomeric Amyloid Beta-Peptide. *Biochem. J.* **2009**, *421*, 415–423. [CrossRef]
48. Kaye, R.; Sokolov, Y.; Edmonds, B.; McIntire, T.M.; Milton, S.C.; Hall, J.E.; Glabe, C.G. Permeabilization of Lipid Bilayers Is a Common Conformation-Dependent Activity of Soluble Amyloid Oligomers in Protein Misfolding Diseases. *J. Biol. Chem.* **2004**, *279*, 46363–46366. [CrossRef]
49. Cheng, P.N.; Pham, J.D.; Nowick, J.S. The Supramolecular Chemistry of β -Sheets. *J. Am. Chem. Soc.* **2013**, *135*, 5477–5492. [CrossRef] [PubMed]
50. Tycko, R.; Wickner, R.B. Molecular Structures of Amyloid and Prion Fibrils: Consensus versus Controversy. *Acc. Chem. Res.* **2013**, *46*, 1487–1496. [CrossRef] [PubMed]
51. Ke, P.C.; Zhou, R.; Serpell, L.C.; Riek, R.; Knowles, T.P.J.; Lashuel, H.A.; Gazit, E.; Hamley, I.W.; Davis, T.P.; Fändrich, M.; et al. Half a Century of Amyloids: Past, Present and Future. *Chem. Soc. Rev.* **2020**, *49*, 5473–5509. [CrossRef] [PubMed]
52. Riek, R. The Three-Dimensional Structures of Amyloids. *Cold Spring Harb. Perspect. Biol.* **2017**, *9*, a023572. [CrossRef]
53. Diaz-Espinoza, R. Catalytically Active Amyloids as Future Bionanomaterials. *Nanomaterials* **2022**, *12*, 3802. [CrossRef] [PubMed]
54. Chang, H.Y.; Chi, J.T.; Dudoit, S.; Bondre, C.; Van De Rijn, M.; Botstein, D.; Brown, P.O. Diversity, Topographic Differentiation, and Positional Memory in Human Fibroblasts. *Proc. Natl. Acad. Sci. USA* **2002**, *99*, 12877–12882. [CrossRef]
55. Sacco, A.M.; Belviso, I.; Romano, V.; Carfora, A.; Schonauer, F.; Nurzynska, D.; Montagnani, S.; Di Meglio, F.; Castaldo, C. Diversity of Dermal Fibroblasts as Major Determinant of Variability in Cell Reprogramming. *J. Cell Mol. Med.* **2019**, *23*, 4256–4268. [CrossRef] [PubMed]
56. Sriram, G.; Bigliardi, P.L.; Bigliardi-Qi, M. Fibroblast Heterogeneity and Its Implications for Engineering Organotypic Skin Models in Vitro. *Eur. J. Cell Biol.* **2015**, *94*, 483–512. [CrossRef] [PubMed]
57. Driskell, R.R.; Watt, F.M. Understanding Fibroblast Heterogeneity in the Skin. *Trends Cell Biol.* **2015**, *25*, 92–99. [CrossRef]

58. Ahuja, A.K.; Pontiggia, L.; Moehrlen, U.; Biedermann, T. The Dynamic Nature of Human Dermal Fibroblasts Is Defined by Marked Variation in the Gene Expression of Specific Cytoskeletal Markers. *Life* **2022**, *12*, 935. [[CrossRef](#)] [[PubMed](#)]
59. Rittié, L.; Fisher, G.J. Natural and Sun-Induced Aging of Human Skin. *Cold Spring Harb. Perspect. Med.* **2015**, *5*, a015370. [[CrossRef](#)] [[PubMed](#)]
60. Bulbaničková, D.; Díaz-Puertas, R.; Álvarez-Martínez, F.J.; Herranz-López, M.; Barrajón-Catalán, E.; Micol, V. Hallmarks and Biomarkers of Skin Senescence: An Updated Review of Skin Senotherapeutics. *Antioxidants* **2023**, *12*, 444. [[CrossRef](#)]
61. Foo, H.; Mather, K.A.; Thalamuthu, A.; Sachdev, P.S. The Many Ages of Man: Diverse Approaches to Assessing Ageing-Related Biological and Psychological Measures and Their Relationship to Chronological Age. *Curr. Opin. Psychiatry* **2019**, *32*, 130–137. [[CrossRef](#)]
62. Wu, L.; Xie, X.; Liang, T.; Ma, J.; Yang, L.; Yang, J.; Li, L.; Xi, Y.; Li, H.; Zhang, J.; et al. Integrated Multi-Omics for Novel Aging Biomarkers and Antiaging Targets. *Biomolecules* **2021**, *12*, 39. [[CrossRef](#)] [[PubMed](#)]
63. Henney, A.M. The Promise and Challenge of Personalized Medicine: Aging Populations, Complex Diseases, and Unmet Medical Need. *Croat. Med. J.* **2012**, *53*, 207. [[CrossRef](#)] [[PubMed](#)]
64. Beger, R.D.; Dunn, W.; Schmidt, M.A.; Gross, S.S.; Kirwan, J.A.; Cascante, M.; Brennan, L.; Wishart, D.S.; Oresic, M.; Hankemeier, T.; et al. Metabolomics Enables Precision Medicine: “A White Paper, Community Perspective. *Metabolomics* **2016**, *12*, 149. [[CrossRef](#)] [[PubMed](#)]
65. Poonprasartporn, A.; Chan, K.L.A. Live-Cell ATR-FTIR Spectroscopy as a Novel Bioanalytical Tool for Cell Glucose Metabolism Research. *Biochim. Biophys. Acta Mol. Cell Res.* **2021**, *1868*, 119024. [[CrossRef](#)] [[PubMed](#)]

Disclaimer/Publisher’s Note: The statements, opinions and data contained in all publications are solely those of the individual author(s) and contributor(s) and not of MDPI and/or the editor(s). MDPI and/or the editor(s) disclaim responsibility for any injury to people or property resulting from any ideas, methods, instructions or products referred to in the content.